ISSN (Print) 2794-7629
ISSN (Online) 2794- 4549
Received 11/08/2024
Accepted 23/09/2024

FULL PAPER

Individual Recognition Based on Multi-Spectrum Palm Images

Prepared by

A.Prof.Dr.Raid Rafi Omar Al-Nima
Northern Technical University,
Mosul, Iraq
raidrafi1@gmail.com

Marwan Khaleel Majeed ALali
Northern Technical University,
Mosul, Iraq
marwankh1970@ntu.edu.iq

Saif Saaduldeen Ahmed
Al-Imam Al-Adham University College
Nineveh, Iraq
syfesaad@gmail.com

Abstract:

Individual recognition based on palm images is such an interesting subject. In this paper, multi-spectrums for full-palm images are considered. The spectra of 460nm and 940nm are employed. Each spectrum provides special features. That is, the spectrum of 460nm affords full-palm textures, and the spectrum of 940nm presents full-palm veins. These facilities are utilized here, where an Artificial Intelligence (AI) approach is suggested. The suggested approach consists of four Deep Learning (DL) networks. Each network is determined for a certain full-palm image, as there are four types of images: right hand full-palm textures, left hand full-palm textures, right-hand full-palm veins, and left-hand full-palm veins. Then, the outputs are fused to provide the final recognition decision. Two datasets are exploited; both are from the Chinese Academy of Sciences Institute of Automation's (CASIA) Multi-Spectral Palmprint Image Database (version. 1.0), where full-palm images of the two spectra 460nm and 940nm are obtained. High performances are achieved after applying the suggested approach.

Keywords: *Deep Learning, Full-Palm Images, Multi-spectrums, Textures, Veins*

المستخلص:

يعد التعرف الفردي بناءً على صور راحة اليد موضوعًا مثيرًا للاهتمام. في هذه الدراسة، تم الأخذ بنظر الاعتبار أطياف متعددة لصور راحة اليد الكاملة. تم استخدام الأطياف 460 نانومتر و 940 نانومتر. يوفر كل طيف ميزات خاصة. أي أن طيف 460 نانومتر يُوفر نسيج راحة اليد الكاملة وطيف 940 نانومتر يُظهر أوردة راحة اليد الكاملة. تم استخدام هذه الخصائص هنا حيث تم اقتراح اسلوب للذكاء الاصطناعي (AI). يتكون الاسلوب المقترح من أربعة شبكات تعلم عميق (DL). تم تحديد كل شبكة لصورة راحة يد كاملة معينة حيث توجد أربعة أنواع من الصور لـ: نسيج راحة اليد الكاملة لليد اليمنى، نسيج راحة اليد الكاملة لليد اليسرى، أوردة راحة اليد الكاملة لليد اليمنى وأوردة راحة اليد الكاملة لليد اليسرى. بعد ذلك، تم دمج المخرجات معًا من أجل الحصول على قرار التمييز النهائي. تم استغلال مجموعتين للبيانات، كلاهما من قاعدة بيانات صور بصمات راحة اليد متعددة الأطياف التابعة لمعهد الأتمتة للأكاديمية الصينية للعلوم (CASIA) (الإصدار 1.0)، حيث تم الحصول على صور راحة اليد الكاملة للطيفين 460 نانومتر و940 نانومتر. تم تحقيق نتائج عالية بعد تنفيذ الاسلوب المقترح.

كلمات مفتاحية: *التعلم العميق، صور لراحة الكف الكاملة، أطياف متعددة، أنسجة، أوردة*

1. INTRODUCTION

The palm is a significant part of the human hand; it is located in the opposite direction of the hand dorsal. It has rich characteristics that each can be used as a valuable biometric. The full palm refers to the inner surface of a hand, including the inner surfaces of five fingers.

The whole inner surface area of a hand, the full palm, has useful characteristics that can be considered for recognition. There are two main characteristics: textures and veins. Such characteristics can be obtained by using determined spectra (lights) (Hao et al., 2007, 2008). For example, the spectrum of 460nm reveals the textures, and the spectrum of 940nm provides the veins (Al-Kaltakchi et al., 2018; Al-Nima, 2017). Figures 1 and 2 show demonstrations for these two characteristics in images from the CASIA Multi-spectral Palmprint Image (CMPI) database (Version 1.0).

In the literature, multiple studies were presented for individual recognition based on the inner surface of palm and finger images. In 2019, a texture recognition study by contactless finger and palmprint was provided. A combination approach of deep learning was proposed. Convolutional Neural Networks (CNN) were utilized to perform the combination between the inner finger texture and palmprint for one hand (Genovese et al., 2019). In the same year, palm images of multispectral were exploited. Face images were reproduced. Multi-fusion methods were utilized (Al-Nima et al., 2019). In 2020, a review for recognizing palm veins was presented. It included a wide survey of prior researches for palm veins in the case of recognition. It also involved basic information, acquiring data, a common dataset, processing, feature collection, and classification. Additionally, there was concentrating on related fusion too (Wu et al., 2020). In 2021, images of palm textures were used for verification. A special deep learning network was proposed. The deep learning network was confirmed after many experiments (Albak et al., 2021). In 2022, the latest advancements were illustrated for

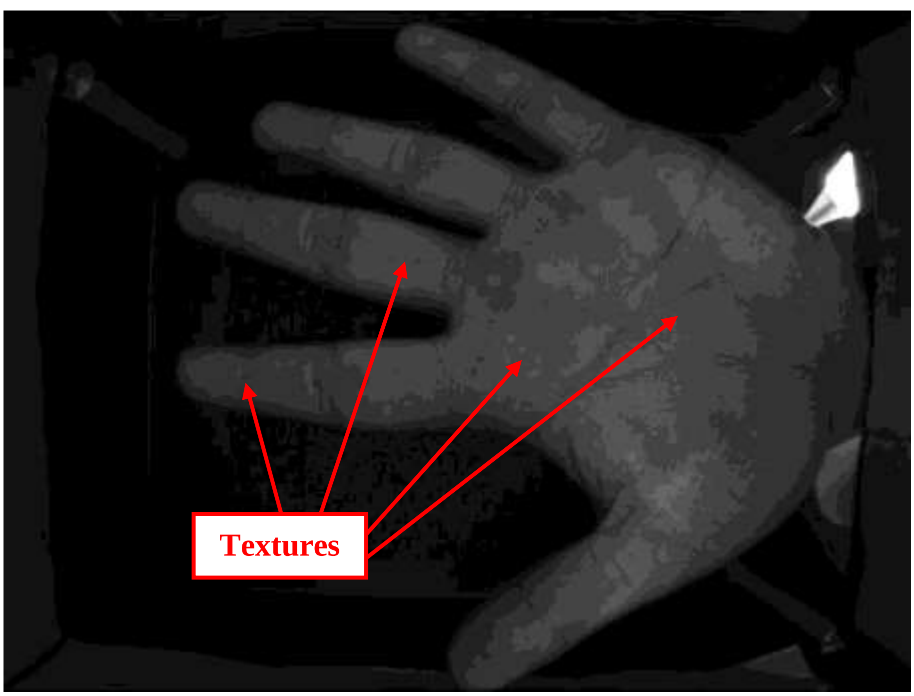

Figures 1: Demonstrations for full-palm textures from the database of CMPI (*CASIA-MS-PalmprintV1*., n.d.)

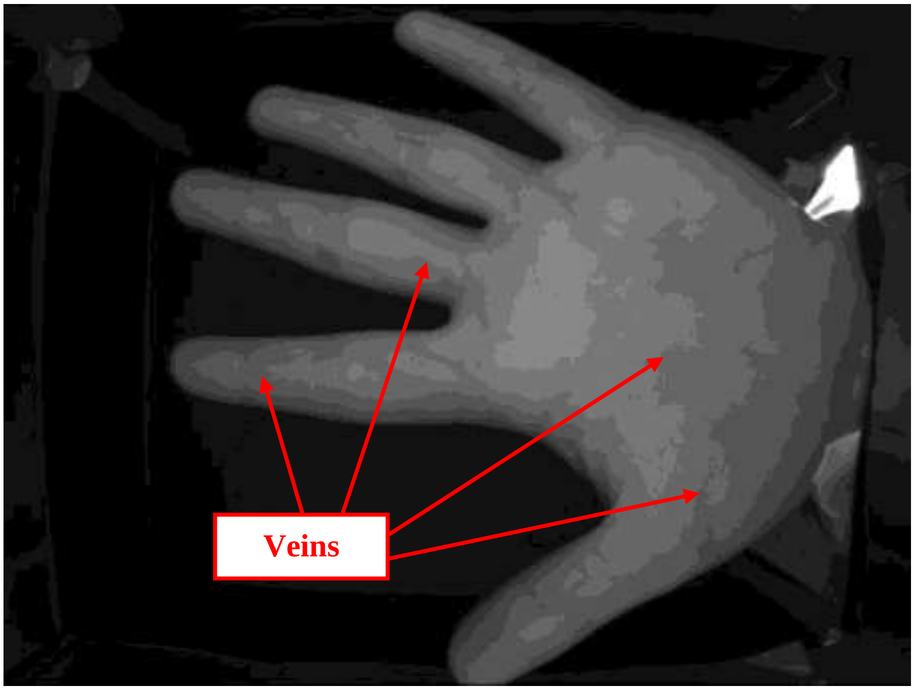

Figures 2: Demonstrations for full-palm veins from the database of CMPI (*CASIA-MS-PalmprintV1.*, n.d.)

finger veins. The case of recognition was considered. Chances, difficulties, and methodology were discussed (Shaheed et al., 2022). In 2024, lightweight CNN was utilized. Palm veins were used for the recognition purpose. Multispectral and contactless existences were taken into account (Teotia & Bansal, 2024).

This paper considers full-palm images for individual recognition. It also introduces an Artificial Intelligence (AI) approach that fuses palm images acquired under multi-spectrums. It exploits two full-palm characteristics: textures and veins.

The paper's sections are as follows: Section 1 introduces general information. Section 2 reveals the suggested approach method. Section 3 demonstrates practical results. and Section 4 summarizes the paper.

2. SUGGESTED APPROACH

In this paper, we propose a comprehensive approach. Individual recognition uses four types of full-palm images as follows:

- Full-palm textures image of a left hand for the acquisition wavelength of 460nm.
- Full-palm texture image of a right hand for the acquisition wavelength of 460nm.
- Full-palm vein image of a left hand for the acquisition wavelength of 940nm.
- Full-palm vein image of a right hand for the acquisition wavelength of 940nm.

The Scholar Journal for Sciences & Technology sjst

Each one of such images is preprocessed and analyzed by a Deep Learning (DL) network. Then, the outcomes of all networks are combined for obtaining the recognition output. Figure 3 shows a demonstration of the suggested approach.

This figure shows that there are multiple stages in the proposed approach. The first stage is for inputting four full-palm images of a single individual, where both hands (right and left) are used and two acquisition wavelengths (460 nm and 940 nm) are employed. The second stage involves preprocessing. That is, each inputted full-palm image is preprocessed by using advised augmentation and resizing operations. Table 1 exposes the advised augmentation operations.

This table illustrates the number of augmentation operations advised to use. These are the color processing, random reflection, random rotation, and random translation. The table shows that every operation has a determined parameter or parameters. Consequently, the resizing operation is considered, where any augmented image is resized to 128×128 pixels. Such operation is useful in further size reduction of employed images, which helps in speeding up the next stage analysis work.

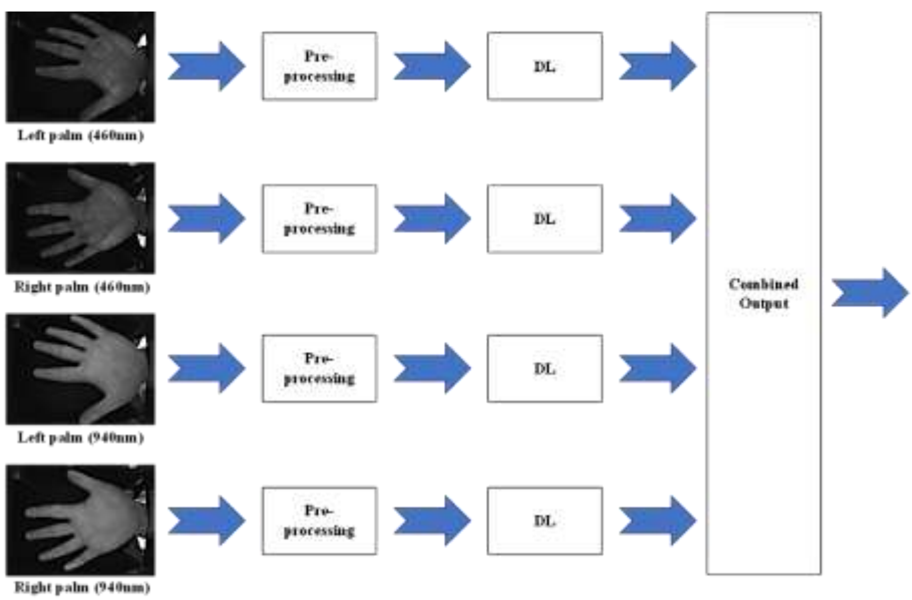

Figure 3: Demonstration of the suggested approach

Table 1: Pre-processing of the advised augmentation operations

Augmentation's No.	Augmentation's Name	Parameter(s)
1	Color processing	Converting from grayscale to RGB (if needed)
2	Random reflection	Probability = 50%

3	Random rotation	Rotation range = [-20°, 20°]
4	Random translation	Horizontal translation range = [-5, 5] and vertical translation range = [-5, 5]

The third stage is for DLs analysis. This stage involves 4 DL networks. All of them have the same advised structure. The name of each network is known as the Convolutional Neural Network (CNN). CNN is a famous DL technique that has been used in many fields such as medical (Arena et al., 2003; Kayalibay et al., 2017), engineering (Sharma et al., 2023; Zhong, 2024), physics (Pistellato et al., 2021; Wei & Chen, 2019), chemistry (Hirohara et al., 2018; Meyer et al., 2019), and industry (Y. Hu et al., 2019; Medus et al., 2021). Here, the advised CNN structure is detailed in Table 2.

Table 2: Details of the advised CNN structure

Layer's No.	Layer's Name	Parameter(s)
1	Image Input	Image size = 128×128 pixels
2	Convolution	Filter size = 3×3 pixels, no. of filters = 32 filters, stride size = 1×1 pixel and padding mode = same as input
3	Rectified Linear Unit (ReLU)	ReLU activation function
4	Pooling	Pooling type = maximum, pooling size = 2×2 pixels and stride size = 2×2 pixels
5	Convolution	Filter size = 3×3 pixels, no. of filters = 64 filters, stride size = 1×1 pixel and padding mode = same as input
6	ReLU	ReLU activation function
7	Pooling	Pooling type = maximum, pooling size = 2×2 pixels and stride size = 2×2 pixels
8	Convolution	Filter size = 3×3 pixels, no. of filters = 128 filters, stride size = 1×1 pixel and padding mode = same as

		input
9	ReLU	ReLU activation function
10	Pooling	Pooling type = maximum, pooling size = 2×2 pixels and stride size = 2×2 pixels
11	Fully connected	No. of nodes = 256neurons
12	ReLU	ReLU activation function
13	Fully connected	No. of nodes = 100 neurons
14	Softmax	Softmax activation function and No. of nodes = 100 neurons
15	Classification	No. of nodes = 100 neurons

So, it consists of 1 image input layer, 3 convolution layers, 4 ReLU layers, 3 pooling layers, 2 fully connected layers, 1 softmax layer, and 1 classification layer. Table 2 provides the parameters of these layers and their sequences. Essentially, any CNN works in one of two phases: learning and evaluation. In the learning phase, the network recognizes samples of images. In the evaluation phase, the network uses what it learns to evaluate other images (G. Hu et al., 2015).

The fourth stage involves the combinations between the outcomes of DLs. There are multiple types of combinations based on the applied rules (Al-Kaltakchi et al., 2018). In this work, the OR rule combination type is considered as the rule that proves its effectiveness (Al-Nima et al., 2020). Subsequently, the recognition output is collected after applying the combination.

3. PRACTICAL RESULTS

First of all, and as mentioned, the CMPI database (Version 1.0) (*CASIA-MS-PalmprintV1.*, n.d.) is exploited. This database consists of multi-spectral full-palm images where six spectra are used in the acquisitions. These are the white, 850nm, 940nm, 630nm, 700nm, and 460nm illuminations. They provide two types of characteristics: textures and veins. A total of 100 individuals participated; each individual allowed capturing six full-palm images for each hand and acquisition illumination (*CASIA-MS-PalmprintV1.*, n.d.).

This study uses only the 460 nm and 940 nm spectra. The 460nm reveals textures, while, the 940nm exposes veins (Al-Nima, 2017). The overall number of images that have been used here is 2400 images of full palms, 1200 images for both spectrums and 1200 images for both hands.

Each set of images for determined illumination and hand is partitioned into 75% for the learning phase and 25% for the evaluation phase. Moreover, the same parameters of the provided training options are assigned to any utilized DL as given in Table 3.

The Scholar Journal for Sciences & Technology sjst

Learning performances show successful achievements. Figures 4, 5, 6, and 7 reveal the performances of learning curves for all 4 DLs, where 1st DL is for left full-palms with the 460nm, 2nd DL is for right full-palms with the 460nm, 3rd DL is for left full-palms with the 940nm, and 4th DL is for right full-palms with the 940nm.

There are two types of learning curves, as seen in these figures. The upper curves expose the relations between the accuracy and iterations. The lower curves expose the relations between the losses and iterations. Each curve approves the learning accomplishment either by increasing accuracy or decreasing loss.

Table 3: Provided training options and parameters that are assigned to any DL

Index	Training options	Parameter(s)
1	Optimizer	Optimizer type = Stochastic Gradient Descent with Momentum (SGDM)
2	No. of epochs	Maximum epochs = 20
3	Initial learning rate	1×10^{-3}
4	Mini batch size	Mini batch size = 64
5	Shuffle	Every epoch
6	Verbose	False

Figure 4: 1st DL learning curves for left full-palms with 460nm acquisition

Figure 5: 2nd DL learning curves for right full-palms with 460nm acquisition

Figure 6: 3rd DL learning curves for left full-palms with 940nm acquisition

Figure 7: 4th DL learning curves for right full-palms with 940nm acquisition

For evaluation, the achievements of each DL and overall combination (the suggested approach) are comprehensively considered. That is, multiple evaluation metrics are taken into account, namely: accuracy, sensitivity, specificity, precision, and f1-score. Table 4 shows comparison of evaluations for each DL and suggested approach.

This table shows that there are multiple achievements to be discussed. 1st DL attains 99.12%, 56.00%, 99.56%, 56.00%, and 56.00% for the accuracy, sensitivity, specificity, precision, and f1-score, respectively. 2nd DL obtains 99.04%, 52.00%, 99.52%, 52.00%, and 52.00% for the same metrics of accuracy, sensitivity, specificity, precision, and f1-score, respectively. 3rd DL achieves 99.02%, 51.00%, 99.51%, 51.00%, and 51.00% also for the same metrics of accuracy, sensitivity, specificity,

Table 4: Comparison of evaluations for each DL and suggested approach

Method	Metrics				
	Accuracy(%)	Sensitivity(%)	Specificity(%)	Precision(%)	F1-score(%)
1st DL (for left full-palms with 460nm)	99.12	56.00	99.56	56.00	56.00
2nd DL (for right full-palms with 460nm)	99.04	52.00	99.52	52.00	52.00
3rd DL (for left full-palms with 940nm)	99.02	51.00	99.51	51.00	51.00
4th DL (for right full-palms with 940nm)	98.96	48.00	99.47	48.00	48.00
Suggested approach (for DLs combination)	99.87	87.00	100	100	93.05

precision, and f1-score, respectively. 4th DL yields 98.96%, 48.00%, 99.47%, 48.00%, and 48.00% again for the same metrics of accuracy, sensitivity, specificity, precision, and f1-score, respectively.

Clearly, our suggested approach benchmarks the highest evaluations of 99.87%, 87.00%, 100%, 100%, and 93.05% for the accuracy, sensitivity, specificity, precision, and f1-score, respectively. It overcomes other DLs in their separate work. It especially has further enhanced the evaluations of sensitivity, precision and f1-score. So, it has recorded significant achievements.

4. CONCLUSION

To conclude, this paper considered individual recognition using multi-spectrum full-palm images. It contributed with a suggested approach. This approach consisted of four stages. The 1st stage was determined for the input full-palm images, where for a single person, both hands of right and left were utilized and two acquisition wavelengths of 460nm and 940nm were exploited. The 2nd stage was assigned for using pre-processing operations of advised augmentation and resizing operations. The 3rd stage was determined for applying an advised DL network with its provided training options four times, where 4 DLs were employed. The 4th stage was assigned for implementing a combination between all outcomes of DLs. The recognition outputs were obtained from the last stage.

The results showed such attractive performances. Learning curves yield acceptable accomplishment. Evaluation values for multiple metrics reveal interesting achievements. The suggested approach attained the highest results of 99.87%, 87.00%, 100%, 100% and 93.05% for the accuracy, sensitivity, specificity, precision, and f1-score, respectively. It significantly further improved the values of sensitivity, precision, and f1-score.

Acknowledgment:

" *Portions of the research in this paper use the CASIA-MS-PalmprintV1 collected by the Chinese Academy of Sciences' Institute of Automation (CASIA)* ".

References:

Al-Kaltakchi, M. T., Omar, R. R., Abdullah, H. N., Han, T., & Chambers, J. A. (2018). Finger texture verification systems based on multiple spectrum lighting sensors with four fusion levels. *Iraqi Journal of Information and Communication Technology*, *1*(3), 1–16.

Al-Nima, R. R. O. (2017). *Signal Processing and Machine Learning Techniques for Human Verification Based on Finger Textures*. Newcastle University.

Al-Nima, R. R. O., Al-Ridha, M. Y., & Abdulraheem, F. H. (2019). Regenerating face images from multi-spectral palm images using multiple fusion methods. *Telkomnika (Telecommunication Computing Electronics and Control)*, *17*(6). https://doi.org/10.12928/TELKOMNIKA.v17i6.12857

Al-Nima, R. R. O., Hasan, S. Q., & Esmail, S. (2020). Exploiting the deep learning with fingerphotos to recognize people. *International Journal of Advance Science and Technology*, *29*(7), 13035–13046.

Albak, L. H., Al-Nima, R. R. O., & Salih, A. H. (2021). Palm print verification based deep learning. *TELKOMNIKA (Telecommunication Computing Electronics and Control)*, *19*(3), 851–857.

Arena, P., Basile, A., Bucolo, M., & Fortuna, L. (2003). Image processing for medical diagnosis using CNN. *Nuclear Instruments and Methods in Physics Research Section A: Accelerators, Spectrometers, Detectors and Associated Equipment*, *497*(1), 174–178.

CASIA-MS-PalmprintV1. (n.d.). http://Biometrics.Idealtest. Org/.

Genovese, A., Piuri, V., Scotti, F., & Vishwakarma, S. (2019). Touchless palmprint and finger texture recognition: A deep learning fusion approach. *2019 IEEE International Conference on Computational Intelligence and Virtual Environments for Measurement Systems and Applications (CIVEMSA)*, 1–6.

Hao, Y., Sun, Z., & Tan, T. (2007). Comparative studies on multispectral palm image fusion for biometrics. *Asian Conference on Computer Vision*, 12–21.

Hao, Y., Sun, Z., Tan, T., & Ren, C. (2008). Multispectral palm image fusion for accurate contact-free palmprint recognition. *2008 15th IEEE International Conference on Image Processing*, 281–284.

Hirohara, M., Saito, Y., Koda, Y., Sato, K., & Sakakibara, Y. (2018). Convolutional neural network based on SMILES representation of compounds for detecting chemical motif. *BMC Bioinformatics*, *19*, 83–94.

Hu, G., Yang, Y., Yi, D., Kittler, J., Christmas, W., Li, S. Z., & Hospedales, T. (2015). When face recognition meets with deep learning: an evaluation of convolutional neural networks for face recognition. *Proceedings of the IEEE International Conference on Computer Vision Workshops*, 142–150.

Hu, Y., Zhang, D., Cao, G., & Pan, Q. (2019). Network data analysis and anomaly detection using CNN technique for industrial control systems security. *2019 IEEE International Conference on Systems, Man and Cybernetics (SMC)*, 593–597.

Kayalibay, B., Jensen, G., & van der Smagt, P. (2017). CNN-based segmentation of medical imaging data. *ArXiv Preprint ArXiv:1701.03056*.

Medus, L. D., Saban, M., Francés-Víllora, J. V, Bataller-Mompeán, M., & Rosado-Muñoz, A. (2021). Hyperspectral image classification using CNN: Application to industrial food packaging. *Food Control*, *125*, 107962.

Meyer, J. G., Liu, S., Miller, I. J., Coon, J. J., & Gitter, A. (2019). Learning drug functions from chemical structures with convolutional neural networks and random forests. *Journal of Chemical Information and Modeling*, *59*(10), 4438–4449.

Pistellato, M., Bergamasco, F., Torsello, A., Barbariol, F., Yoo, J., Jeong, J.-Y., & Benetazzo, A. (2021). A physics-driven CNN model for real-time sea waves 3D reconstruction. *Remote Sensing*, *13*(18), 3780.

Shaheed, K., Mao, A., Qureshi, I., Kumar, M., Hussain, S., & Zhang, X. (2022). Recent advancements in finger vein recognition technology: methodology, challenges and opportunities. *Information Fusion*, *79*, 84–109.

Sharma, S. P., Singh, L., & Tiwari, R. (2023). Design of an efficient integrated feature engineering based deep learning model using CNN for customer's review helpfulness prediction. *Wireless Personal Communications*, *133*(4), 2125–2161.

Teotia, K., & Bansal, M. (2024). Using a Lightweight Convolutional Neural Network for Contactless Multispectral Palm-Vein Recognition. *Revista Electronica de Veterinaria*, *25*(1S), 60–75.

Wei, Z., & Chen, X. (2019). Physics-inspired convolutional neural network for solving full-wave inverse scattering problems. *IEEE Transactions on Antennas and Propagation*, *67*(9), 6138–6148.

Wu, W., Elliott, S. J., Lin, S., Sun, S., & Tang, Y. (2020). Review of palm vein recognition. *IET Biometrics*, *9*(1), 1–10.

Zhong, M. (2024). Risk early warning model of tunnel engineering based on computer vision and CNN. *Journal of Physics: Conference Series*, *2816*(1), 12026.